JOURNAL OF MATERIALS SCIENCE 26 (1991) 621–630

Single and multi-specimen *R*-curve methods for J_{IC} determination of toughened nylons

S. HASHEMI*, J. G. WILLIAMS
Mechanical Engineering Department, Imperial College of Science, Technology and Medicine, London SW7 2BX, UK

For characterization of the fracture resistance of materials used in the upper shelf toughness regime, *J–R* curves are widely considered the most promising candidates. However, there still remain problems concerning both the generation and measurement of *J–R* curves as material characterizing parameters and their application in ductile fracture analyses for failure prediction in polymeric materials. This paper reports the results of investigations conducted on two rubber-toughened nylons at room temperature. Two different methods of *J–R* curve determination are covered, namely multi-specimen and single specimen test methods. The resulting *J–R* curves have also been evaluated to obtain values of the initiation toughness, J_{IC}, following the extrapolation and interpolation schemes prescribed by ASTM E813-81 and ASTM E813-87 test procedures, respectively. The results show that the multiple specimen unloading method and the single specimen partial unloading compliance method can be used to generate comparable crack growth resistance *J–R* curves of the toughened nylons. The value of J_{IC} for the crystalline rubber-toughened nylon was approximately twice the value obtained for the amorphous rubber-toughened nylon. The former material also exhibited a greater resistance to ductile crack growth.

1. Introduction

Polymeric materials are increasingly being used for load-bearing structural applications and, therefore, an understanding of their fracture properties is becoming more important. Linear elastic fracture mechanics (LEFM) has successfully described the fracture properties of brittle polymers (e.g. [1, 2]). The test procedure for determining plane strain fracture toughness, K_{IC}, is well accepted and documented [3]. The main limitation of the test procedure is the minimum size of the specimen that can be tested. According to ASTM [3], plane strain conditions at the crack tip are achieved when the following minimum size requirements are met: a, $W - a$, $B \geqslant 2.5(K_{IC}/\sigma_y)^2$ and $W \geqslant 2B$. These specimen size requirements, in effect, limit the size of the crack tip plastic zone relative to the specimen dimensions, because the plastic zone size is proportional to the ratio $(K_{IC}/\sigma_y)^2$. Only when the specimen dimensions are larger than the minimum size prescribed by the above equation can one expect that the plastic zone has a negligible effect on the stresses around the crack tip and thus on the measured value of K_{IC}. For tough polymers the available specimen sizes preclude the measurement of toughness on specimens which are valid for analysis using the concepts of linear elastic fracture mechanics, in that significant plastic yielding occurs at the crack tip prior to onset of crack extension. This specimen size limitation has led to the development of the *J*-integral and the crack growth resistance "*R*-curve" approach, which allows the consistent measurement of fracture toughness in much smaller specimens than is possible with the K_{IC} procedure. The critical value of J, J_{IC}, corresponding to a critical amount of Mode I crack growth is the quantity of interest in J_{IC} testing.

One method that has been recommended for evaluation of J_{IC} is the multiple specimen *R*-curve method [4, 5]. Evaluation of J_{IC} using this method requires the use of several specimens to establish an R-curve and thereby the J_{IC} value. This procedure has been used by several investigators (e.g. [6–11]), demonstrating that polymers can be characterized by the *J*-integral approach. However, the multi-specimen test procedure is not only time consuming but also requires a large amount of material for test specimens. For these reasons, particularly the limited availability of the material, considerable attention was paid to the development of an alternative test method to define the *R*-curve and thereby the J_{IC} value. Hence, the development of the single specimen *R*-curve method [12–14].

In this paper, the *J*-integral approach is used to characterize the fracture behaviour of two toughened nylons. The main objective is to compare the fracture data of the multi-specimen *R*-curve with that obtained by the single-specimen *R*-curve method. Furthermore, the resulting *R*-curves have been evaluated to determine the values of initiation toughness, J_{IC}, following

* *Present address*: London School of Polymer Technology, Polytechnic of North London, Holloway Road, London N7 8DB, UK.

0022–2461/91 $03.00 + .12

the schemes of the ASTM E813-81 and ASTM E813-87 test procedures.

2. The *J*-integral

The *J*-integral is increasingly used as a fracture parameter for characterization of the elastic–plastic behaviour of engineering materials. While the *J*-integral is an approximate measure of the amplitude of the crack tip stress–strain singularities, it is attractive for fracture characterization because it may be readily evaluated without resorting to detailed, tedious analyses of the crack tip region *per se*. For small-scale yielding, the *J*-integral becomes *G* and is simply related to the familiar stress intensity factor *K* of linear elastic fracture mechanics, and this relationship may provide an economical means of estimating the plane strain fracture toughness K_{IC} from small, often fully plastic, laboratory specimens. (This relationship is currently being de-emphasized in ASTM metals studies.)

The *J*-integral was originally defined as a path-independent line integral for two dimensional problems and can be expressed in terms of energy [15] as

$$J = -\frac{1}{B}\frac{dU}{da} \tag{1}$$

where *U* is the potential energy of the loaded body (the area under the load–loadline displacement curve). Equation 1 was later expressed as [16]

$$J = J_e + J_p \tag{2}$$

where J_e and J_p are the elastic and plastic components of the total *J* value given, respectively, as

$$J_e = \frac{\eta_e U_e}{B(W-a)} \tag{3}$$

and

$$J_p = \frac{\eta_p U_p}{B(W-a)} \tag{4}$$

U_e and U_p are elastic and plastic energy components, respectively, of the total energy, U_T, as shown in Fig. 1. η_e and η_p are their corresponding elastic and plastic work factors. *W* is the specimen width and *a* is the length of the initial crack. The expression for the total *J* value may, therefore, be written as

$$J = \frac{1}{B(W-a)}(\eta_e U_e + \eta_p U_p) \tag{5}$$

The elastic work factor, η_e, can be evaluated for a given specimen geometry from the compliance or from the LEFM shape factor, $Y(a/W)$, and the plastic work factor, η_p, from a limit load analysis. For example, for the three-point bend single-edge notched specimen we have

$$\eta_e = \frac{(W-a)Y^2 a}{\left(\int Y^2 a\, da + \frac{SW}{18}\right)} \tag{6}$$

and

$$\eta_p = \left(\frac{W-a}{WP_L}\right)\frac{\partial P_L}{\partial(a/W)} \tag{7}$$

where P_L is the limit load.

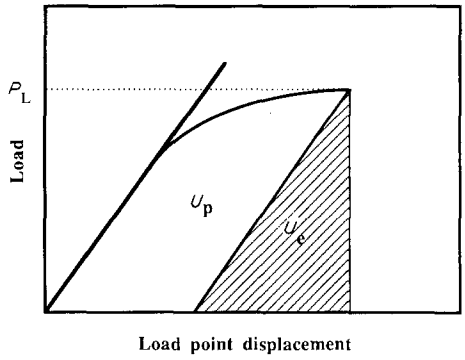

Figure 1 Schematic load–loadpoint displacement curve showing partitioning of elastic and plastic work.

3. Crack growth resistance curve (*R*-curve)

To take account of the growth of cracks, the concept of resistance curves has been developed where either a pseudoelastic *K* or an elastic–plastic *J* is plotted against crack extension. Neither of these concepts is rigorously valid but they do provide a way of defining the amount of energy required to advance the crack.

A simplified curve of *J* against crack growth, Δa, is schematically shown in Fig. 2. The first part with a high slope (blunting line) is developed before initiation when the initial crack is extended only slightly by the geometry of the stretch zone. Crack tip blunting causes the formation of this stretched zone prior to material separation. Assuming the stretched zone size, $(\Delta a)_{sz}$, is equal to half the crack opening displacement, COD, and relating the COD to *J* as $J = (\text{COD})\sigma_y$ (where σ_y is the yield stress of the material), the blunting line may be expressed as $J = 2(\Delta a)_{sz}\sigma_y$. At the initiation point the slope reduces abruptly, reflecting the fact that the resistance to crack extension during the growth period is less than during the initiation period. However, in many materials this change in slope is gradual and a linear resistance curve as shown in Fig. 2 would give a J_{IC} value which is imprecise. Because of this, the ductile crack growth part of the J–Δa curve is generally curve fitted by a power law expression rather than assumed linear: this point will be pursued later when various data qualifying schemes for determining the crack growth resistance curve are examined.

To construct a J–Δa curve two test methods may be adopted as outlined below, depending on whether the Δa values are to be measured physically or to be estimated.

3.1. Multiple specimen *R*-curve method

The multiple specimen method was originally proposed by Landes and Begley [17]. In this method, identical specimens are loaded monotonically to various values of loadpoint displacement to obtain different levels of crack growth and then fully unloaded. After unloading, the specimens are broken open for direct measurement of crack extensions, Δa. The *J*-value for each specimen is calculated from the measured area under the load–loadline displacement curve using Equation 2 with appropriate values of η_e and

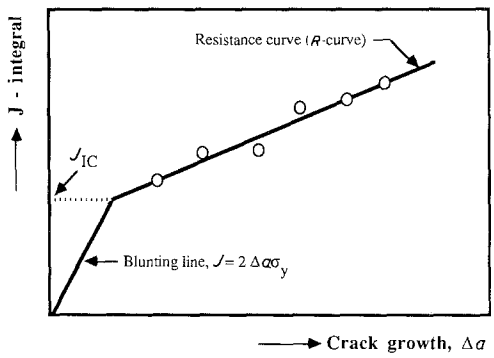

Figure 2 Schematic J-integral–crack extension, Δa, curve.

η_p. The crack growth resistance curve is then constructed by plotting the J-values against the corresponding Δa values.

3.2. Single specimen R-curve method (partial unloading compliance)

During this fracture test a specimen is partially unloaded frequently. The compliance at each unloading (compliance, $C = \delta/P$) is then used to determine the crack length and the amount of crack extension.

Using a transfer function, δ_{cm}, for the inverse crack-mouth compliance of a three-point bend specimen as proposed by Kapp *et al.* [18]

$$\delta_{cm} = \frac{1}{1 + \left(\frac{3.95S/W}{E'BC_{cm}}\right)^{1/2}} \quad (8)$$

the relative crack depth (a/W) may be expressed as a fifth order polynomial of this transfer function as [19]

$$\frac{a}{W} = 9.56 \times 10^{-4} + 5.504 \times 10^{-2}\delta_{cm} - 1.0968\delta_{cm}^2 + 9.9706\,\delta_{cm}^3 - 13.096\delta_{cm}^4 + 5.1707\delta_{cm}^5 \quad (9)$$

where B is the specimen thickness, S the span width, W the specimen width, E' is the effective modulus of elasticity and C_{cm} the crack-mouth compliance given by

$$E'BC_{cm} = \left(\frac{S}{W}\right)\frac{\alpha}{(1-\alpha)^2} \times [8.737 - 8.681\alpha^{0.5} + 3.321\alpha + 0.573\alpha^{1.5}] \quad (10)$$

where $\alpha = a/W$. In the range $0.2 \leqslant a/W \leqslant 0.8$ the error of this approximation is within $\pm 0.25\%$ but this may be improved considerably by the following correction [19]

$$\left(\frac{a}{W}\right)_{\text{corrected}} = \left(\frac{a}{W}\right) + \frac{C_{cm}(\text{exp}) - C_{cm}(a/W)}{dC_{cm}(a/W)/d(a/W)} \quad (11)$$

where $C_{cm}(\text{exp})$ is the experimental value of the crack-mouth compliance at which the crack depth must be determined and $C_{cm}(a/W)$ is the calculated crack-mouth compliance. The crack resistance curve can now be established by plotting J against the corresponding estimated value of Δa. The J-value at each unloading point can be calculated using the following relationship

$$J_k = J_{k-1} + \frac{\eta_e U_{e(k,k-1)}}{B(W-a)} + \frac{\eta_p U_{p(k,k-1)}}{B(W-a)} \quad (12)$$

where $U_{e(k,k-1)}$ is the elastic energy component and (the area under the load–loadline displacement record between lines of constant displacement at two consecutive unloading points k and $k-1$) and $U_{p(k,k-1)}$ is the plastic energy component (the area under the load–loadline displacement record between two consecutive unloading points k and $k-1$).

Note, that the effective modulus of elasticity, E', can be determined from Equation 10 using crack-mouth compliance values of the first few unloading lines where $\Delta a = 0$.

4. ASTM data-qualifying schemes for J_{IC} testing

In order to determine a valid measure of the material fracture toughness, J_{IC}, and to construct an accurate crack growth resistance curve (J–Δa curve), certain validity requirements and data-qualifying schemes were prescribed by the ASTM [4, 5]. The validity requirements are applied to the data in an attempt to ensure specimen size independence so that J_{IC} uniquely characterizes the fracture behaviour of ductile materials. The data-qualifying schemes are also prescribed to ensure a consistent crack growth resistance curve. Figs 3a and b show the two data qualifying schemes that are proposed by the ASTM. A brief summary of the two schemes and the manner in which the J_{IC} value is determined are given below.

4.1. ASTM E813-81 (Fig. 3a)

This version of the standard defines the J–Δa points for the resistance curve as those data points lying between two offset lines each drawn parallel to the blunting line of $J = 2\Delta a\sigma_y$. The minimum offset is 0.6% of the length of the uncracked ligament and the maximum offset being 6% of the length of the uncracked ligament. The resistance curve is then defined by the best linear regression line through the data points within these two exclusion lines. The intersection of the resistance curve with the blunting line gives the J_{IC} value.

4.2. ASTM E813-87 (Fig. 3b)

In this version the standard defines the J–Δa points for the resistance curve as those data points lying between two offset lines each drawn parallel to the blunting line of $J = 2\Delta a\sigma_y$. The minimum offset is 0.15 mm of crack growth and the maximum offset being 1.5 mm of crack growth. It is also required that at least one J–Δa point should lie between the 0.15 mm exclusion line and a parallel line with an offset of 0.5 mm from the blunting line, and one datum point should lie between a line parallel to the blunting line at an offset of 1.0 mm and the 1.5 mm exclusion line. The acceptable data are then curve fitted by a

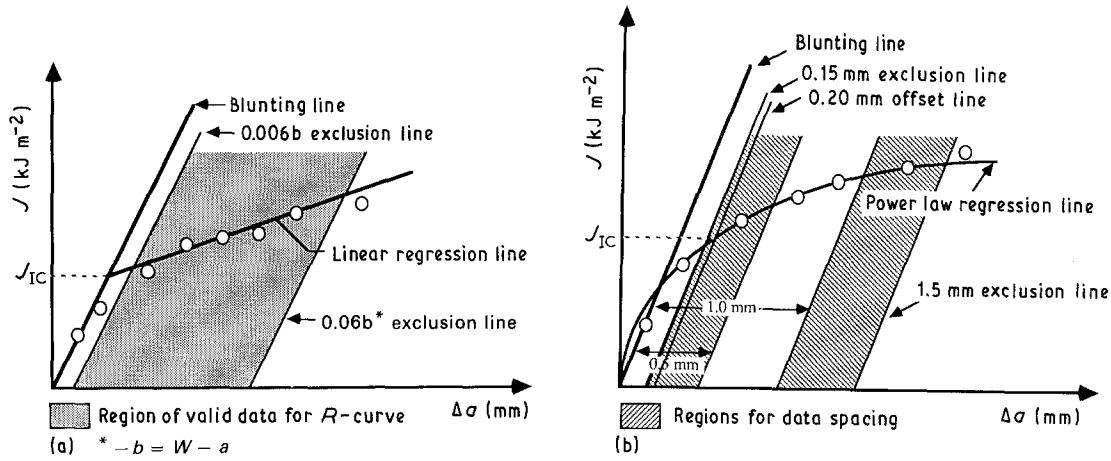

Figure 3 Data-qualifying schemes according to ASTM standard.

power law regression line of the form

$$\ln J = \ln C_1 + C_2 \ln \Delta a \quad (13)$$

The intersection of this power law regression line with a line parallel to the blunting line at an offset of 0.2 mm gives the value of J_{IC}.

4.3. J_{IC} validity requirements

For fracture to be characterized by a J_{IC} value, a specimen must meet certain size requirements in order to achieve a plane-strain stress state along the crack front. To achieve this stress state all specimen dimensions must exceed some multiple of J_{IC}/σ_y. According to ASTM, a valid J_{IC} value may be obtained whenever

$$B,\ (W - a),\ W \geqslant 25(J_{IC}/\sigma_y) \quad (14)$$

and

$$\frac{dJ}{d(\Delta a)} \leqslant \sigma_y \quad (15)$$

(the slope of the power law regression line, $dJ/d(\Delta a)$, is evaluated at $\Delta a = 0.2$ mm). Furthermore, for the J–Δa data to be regarded as a material property independent of specimen size, the criterion $\omega \geqslant 10$ must be met, where ω is defined as

$$\omega = \frac{W - a}{J_{IC}} \frac{dJ}{d(\Delta a)} \quad (16)$$

Finally, for plane strain linear elastic behaviour J_{IC} becomes identical to the critical strain energy release rate, G_{IC}, which is in turn related to the stress intensity factor K_{IC} used in linear elastic fracture mechanics

$$J_{IC} = G_{IC} = \frac{1 - \nu^2}{E} K_{IC}^2 \quad (17)$$

where ν is Poisson's ratio and E is the Young's modulus.

5. Experimental procedure

5.1. Materials

Materials were supplied by Du Pont de Nemours and Company, Inc. in the form of injection-moulded plaques (plaque dimensions were 100 mm × 254 mm × 12.5 mm) made of rubber-toughened crystalline nylon 6/6 (trade name Zytel ST801) and rubber toughened amorphous nylon 6/6 (trade name Zytel ST901).

5.2. Specimen preparation

The specimens were essentially tested dry as-moulded. From each plaque two bend specimens with a width, W, of 30 mm, thickness, B, of 12.5 mm and length, L, of 150 mm were cut as shown in Fig. 4. All the specimens were deeply notched to $a/W = 0.50$ in the direction shown in Fig. 4, using a fly cutter of tip radius of 12 μm.

5.3. Test conditions, apparatus and procedure

Specimens were tested in three-point bend at room temperature using the apparatus shown schematically in Fig. 5. A screw-driven Instron machine was used to apply the load and was operated at a constant displacement rate of 2 mm min^{-1}. All the specimens were tested using a span-to-specimen width ratio, S/W, of 4:1.

5.3.1. Multiple specimen method

A continuous plot of load–loadline displacement was obtained for each specimen using an X–Y chart recorder. Sixteen specimens were tested for each material and each specimen was loaded to a different value of loadpoint displacement and then unloaded. The loadline displacement was measured using an

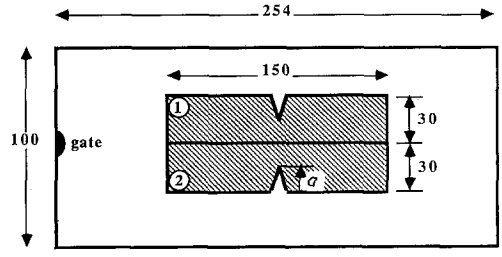

Figure 4 J specimens. All dimensions in millimetres.

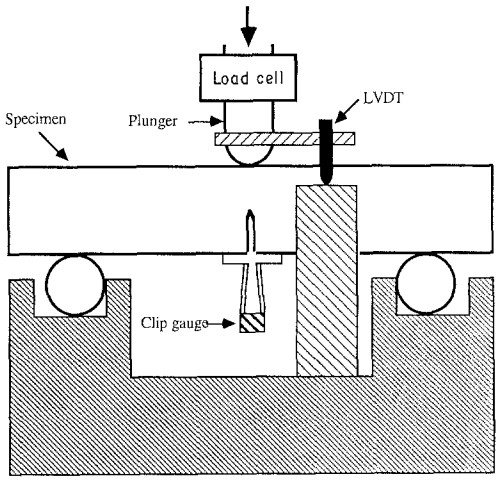

Figure 5 Three-point bend fixture and associated gauges.

LVDT which was secured to the load plunger and the support base as shown schematically in Fig. 5. After unloading, each specimen was submerged in liquid nitrogen for 2 min and then put back in the test machine and fractured in a brittle manner so that the crack extension could be measured. Different amounts of crack growth were observed on each specimen due to unloading at different displacement levels. The length of the initial crack and crack extension was measured using a X10 travelling microscope.

5.3.2. Single specimen method

Crack-mouth opening and the loadline displacement were simultaneously recorded as a function of the applied load using two X–Y chart recorders. For crack-mouth opening measurement a clip gauge was clipped to knife edges attached to the tension surface of the specimen (see Fig. 5). An LVDT was used to measure the loadline displacement as before. Two to three specimens were tested for each material. Each specimen was loaded and partially unloaded several times in order to generate sufficient J–Δa points to develop an acceptable J–R curve as defined by the standards. The unload/reload cycles were conducted at a displacement rate of 2 mm min^{-1} and the unloading range was approximately 20% to 30% of the current load value. After the final unloading the load was reduced to zero and the specimen was broken open and the extent of the final ductile crack growth was measured.

6. Results and discussion

6.1. K_Q analysis

Figs 6a and b show typical P–loadline displacement diagrams for precracked Zytel ST801 and Zytel ST901 specimens, respectively. The amount of crack extension Δa (as revealed by the unload–liquid nitrogen procedure) at several positions on the curves is also indicated on the two diagrams. Also shown is the load P_Q, defined by ASTM E399-78 as the load corresponding to a 5% secant offset on the curve of P–loadline displacement. This load is used to calculate a K_Q value which in turn may be regarded as a valid K_{IC} number provided that the amount of plasticity at P_Q is small and the rate of crack extension above P_Q is rapid, i.e.

$$B, a_0, W - a_0 > 2.5\left(\frac{K_Q}{\sigma_y}\right)^2 \quad (18)$$

$$\frac{P_{max}}{P_Q} < 1.10 \quad (19)$$

where P_{max} represents the maximum load sustained in the test and σ_y is the yield strength. As summarized in Table I neither of these criteria is met for any of the materials considered here. Examination of Figs 6a and b also reveals that P_Q falls significantly below the load level at which the true crack extension was first observed. At P_Q the amount of crack extension is zero and these considerations demonstrate conclusively that K_Q cannot be meaningfully employed for fracture characterization in Zytel ST801 or Zytel ST901 using the present specimen sizes.

6.2. J_{IC} analysis

6.2.1. Multi-specimen results

Figs 6a and b show that crack extension commences below P_{max} and that initial crack growth is not accompanied by a well-defined discontinuity on the P–loadline displacement curve. For both materials, initial growth began near the specimen mid-thickness where the transverse constraint is maximized. Upon further loading the crack-front assumed an elliptical shape with relatively little extension apparent at the specimen surface. At the higher loads the familiar "thumbnail" shape was observed. In this study crack growth was measured at the centre of the fracture surface which corresponded to the maximum amount of crack extension in the specimen. The area under the

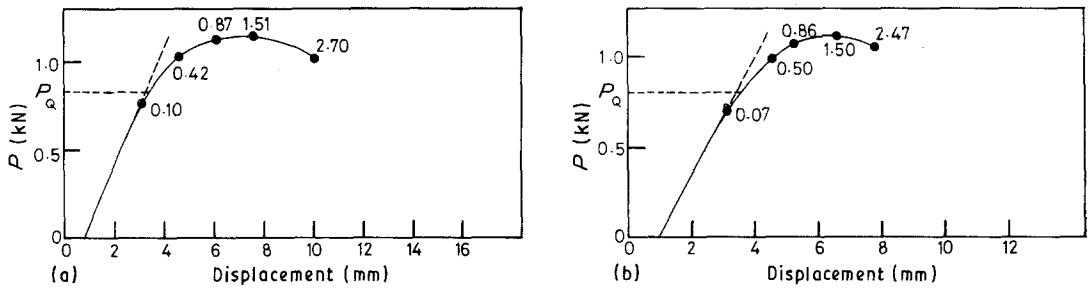

Figure 6 Typical load–loadline displacement curves for (a) Zytel ST801 and (b) Zytel ST901. The amount of crack extension, Δa (mm) (as revealed by the unload–liquid nitrogen procedure) at several positions on the curves is also indicated on the two diagrams.

TABLE I Fracture toughness results for Zytel ST901 and Zytel ST801

Material	B (mm)	W (mm)	a_o (mm)	P_{max}/P_Q	K_Q (MPa $m^{1/2}$)	$2.5(K_Q/s_y)^2$ (mm)
Zytel ST901	12.42	30.33	16.03	1.39	4.26	16.78
Zytel ST801	12.30	30.02	15.22	1.37	4.20	25.00

load–displacement curves was measured by a graphical integration method (i.e. Simpson's rule). Recall that the specimens were notched to half their width ($a/W = 0.5$) and were tested with a span of $4W$. Under these conditions we have $\eta_e = \eta_p = 2$ [4, 5] so that Equation 5 can be reduced to the more simple form of

$$J = \frac{2U_T}{B(W-a)} \tag{20}$$

The values of J calculated according to Equation 20 are plotted against crack extension, Δa, in Figs 7a, b and 8a, b for Zytel ST801 and Zytel ST901 respectively. In Figs 7a and 8a, R-curves are constructed according to the ASTM E813-81 test procedure, whereas in Figs 7b and 8b the same J–Δa values are plotted but R-curves are constructed in accordance with the current ASTM E813-87 test procedure. The following observations can be made about the general behaviour of the J–R curves: (i) J–Δa points show very little scatter; (ii) data point spacing satisfies the ASTM requirements (E813-81 and E813-87) extremely well; and (iii) ASTM E813-87 gives a much higher J_{IC} value than the ASTM E813-81. Indeed, the initiation values evaluated from the power law fit to the J–R curves according to ASTM E813-87 are almost twice the values evaluated from a linear fit to the J–R curves according to ASTM E813-81. The increase of $J_{IC,E813\text{-}87}$ over $J_{IC,E813\text{-}81}$ is a consequence of $J_{IC,E813\text{-}87}$ not being evaluated from the real onset of crack growth (as defined by the blunting line) but for a finite amount of stable crack growth (i.e. 0.2 mm). Values of J_{IC} evaluated from the ASTM E813-81 and ASTM E813-87 test procedures are given in Table II. These values agree quite well with the J_{IC} values reported by Huang and Williams [9] testing the same materials.

As may be seen from Table II and as illustrated graphically in Fig. 9, the ductile fracture toughness response of the Zytel ST801 is superior to that of the Zytel ST901. In fact, the J_{IC} value of Zytel ST801 is roughly twice that of Zytel ST901. Furthermore, using the concept of material tearing modulus (T_m) as

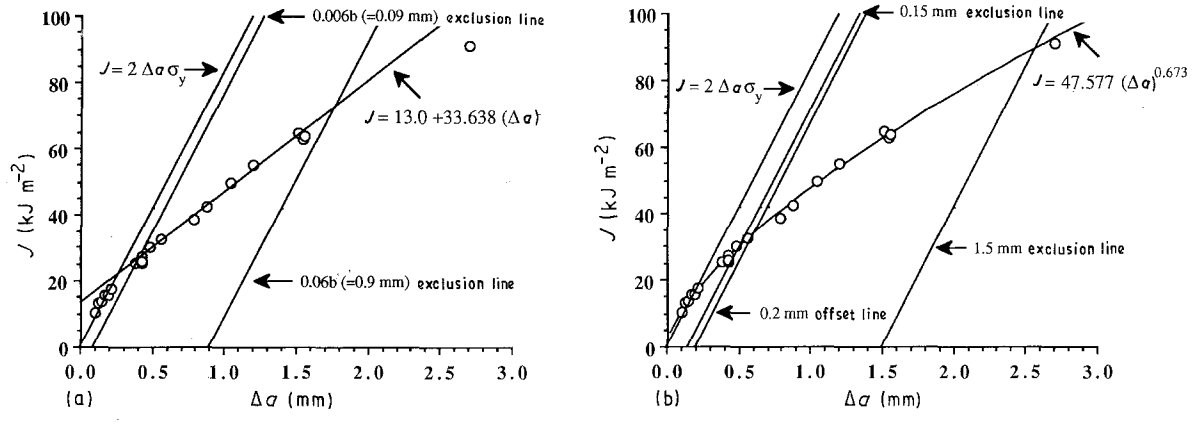

Figure 7 J–Δa curves for Zytel ST801. Data were obtained using the multiple specimen R-curve method, and analysed according to (a) ASTM E318-81, (b) ASTM E318-87.

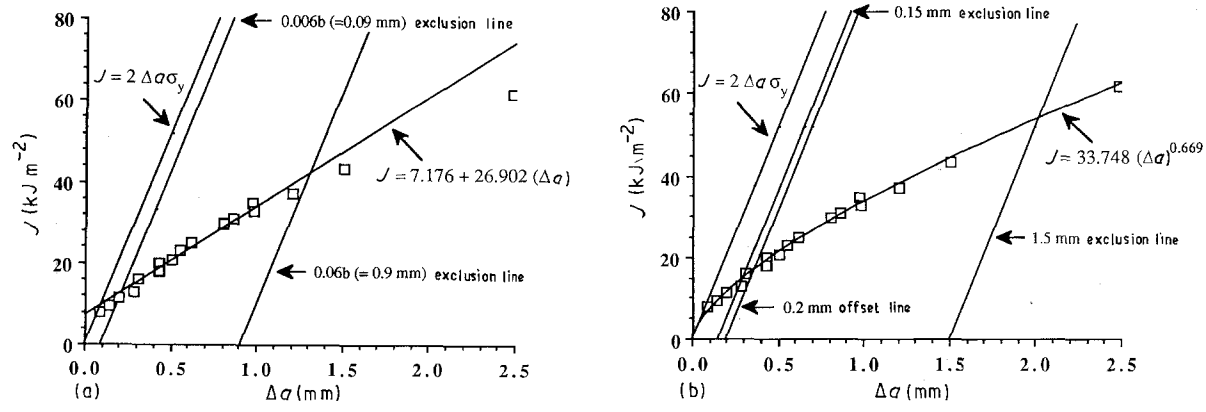

Figure 8 J–Δa curves for Zytel ST901. Data were obtained using the multiple specimen R-curve, and analysed according to (a) ASTM E318-81, (b) ASTM E318-87.

TABLE II Multi-specimen test results for Zytel ST901 and Zytel ST801

Material	Standard	Resistance curve	J_{IC}(kJ m^{-2})
Zytel 901	ASTM E813-81	$J = 7.176 + 26.902\,\Delta a$	9.68
	ASTM E813-87	$J = 33.748(\Delta a)^{0.669}$	17.22
Zytel 801	ASTM E813-81	$J = 13.00 + 33.638\,\Delta a$	21.68
	ASTM E813-87	$J = 47.577(\Delta a)^{0.673}$	33.64

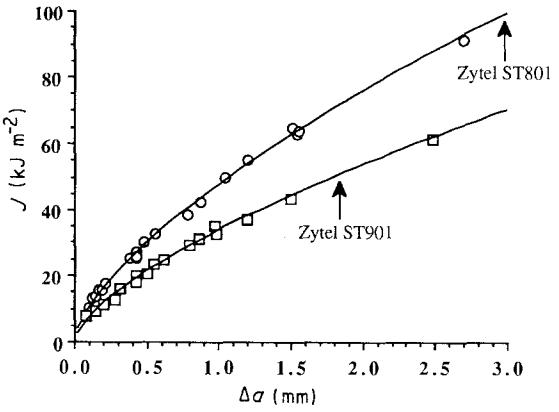

Figure 9 Comparison of Zytel ST901 and Zytel ST801 *R*-curves. Data were obtained by the multiple specimen *R*-curve method.

TABLE III Size requirements for valid J_{IC} and the K_{IC} tests*

Material	J_{IC} (kJ m^{-2})	K_{IC} (MPa m$^{1/2}$)	B_J, W_J† (mm)	B_K, W_K† (mm)
Zytel 901	9.68	4.27	4.65, 9.31	16.86, 33.71
	17.22	5.68	8.28, 16.56	29.83, 59.66
Zytel 801	21.68	6.38	12.90, 25.81	57.77, 115.38
	33.64	7.95	20.02, 40.05	89.57, 179.15

*The following mechanical properties were used in the calculations:
(i) for Zytel 901: $\sigma_y = 52$ MPa, $E = 1.88$ GPa;
(ii) for Zytel 801: $\sigma_y = 42$ MPa, $E = 1.88$ GPa and with $\nu = 0.3$.
†B_J and W_J are the minimum specimen sizes for J_{IC} test; B_K and W_K are the minimum specimen sizes for K_{IC} test.

TABLE IV Multi-specimen test results for Zytel ST901 and Zytel ST801

Material	Standard	$dJ/d(\Delta a)$ (kJ m^{-3})		σ_y (MPa)	ω
Zytel 901	ASTM E813-81	26.90	<	52	41.69
	ASTM E813-87	38.46	<	52	33.50
Zytel 801	ASTM E813-81	33.64	<	42	23.27
	ASTM E813-87	54.20	>	42	24.16

introduced by Paris *et al.* [20]

$$T_m = \frac{dJ}{d(\Delta a)} \frac{E}{\sigma_y^2} \tag{21}$$

which depends on the slope of the *R*-curve as well as the material yield stress and Young's modulus, we may describe the stability of the crack growth. Using the $dJ/d(\Delta a)$ values obtained by the ASTM E813-81 test procedure (see Table II) we obtain T_m values of 18.70 and 35.85 for Zytel ST901 and Zytel ST801, respectively. This indicates that the former is less resistant to tearing instability once J_{IC} is exceeded. In fact, these variations in J_{IC} and T_m were reflected in the overall shape of the load–loadline displacement curves. For example, as shown in Figs 6a and b, Zytel ST801 exhibits a greater total displacement for a given Δa value, thereby accounting for its superior fracture resistance in comparison to Zytel ST901. It must be pointed out that both materials were stable at all times. This behaviour can be predicted if we consider the condition for unstable tearing as proposed by Paris *et al.* [20]

$$T_m < \frac{2(W-a)^2 S}{W^3} \tag{22}$$

The term on the right-hand side of Equation 22 is called the "applied tearing modulus (T_a)" and thus, for $W = 30$ mm, $W - a = 15$ mm and $S = 120$ mm we have $T_a = 2.00$, i.e. $T_a < T_m$ predicting stable tearing as observed.

The values of plane strain fracture toughness (K_{IC}) for the two materials as derived from J_{IC} are presented in Table III. Minimum specimen size requirements for valid J_{IC} and the K_{IC} tests are also given in Table III. As may be seen, the specimen size employed here is either bigger or very close to the ASTM recommended size for a valid J_{IC} test except for Zytel ST801 where the E813-87 test procedure predicts invalid specimen size. Note also, that if K_{IC} values were measured directly without recourse to J_{IC} testing, the size of the specimen would have to be very large, particularly for Zytel "801", which makes the K_{IC} test impractical for testing such toughened systems.

Finally, results of a detailed investigation into the uniqueness of the *J–R* curves are given in Table IV. As may be seen, conditions given by Equations 14 to 16 are satisfied; that is $dJ/d(\Delta a) < \sigma_y$ and $\omega > 10$, except for Zytel ST801 using the ASTM E813-87 scheme. Recall that the specimen size calculations based on the power law fit to J–Δa points also predicted an invalid J_{IC} test (see Table III).

6.2.2. Single specimen results

In the unloading compliance test, the crack length at each unloading was determined from the unloading compliance of the load–crack-mouth opening displacement curve as required by Equation 11. Typical loading and unloading curves are shown in Figs 10 and 11. Also shown in these figures are the lines from which compliance values were measured and hence Δa values evaluated (the effective modulus of the elasticity, E', was determined from the compliance of the

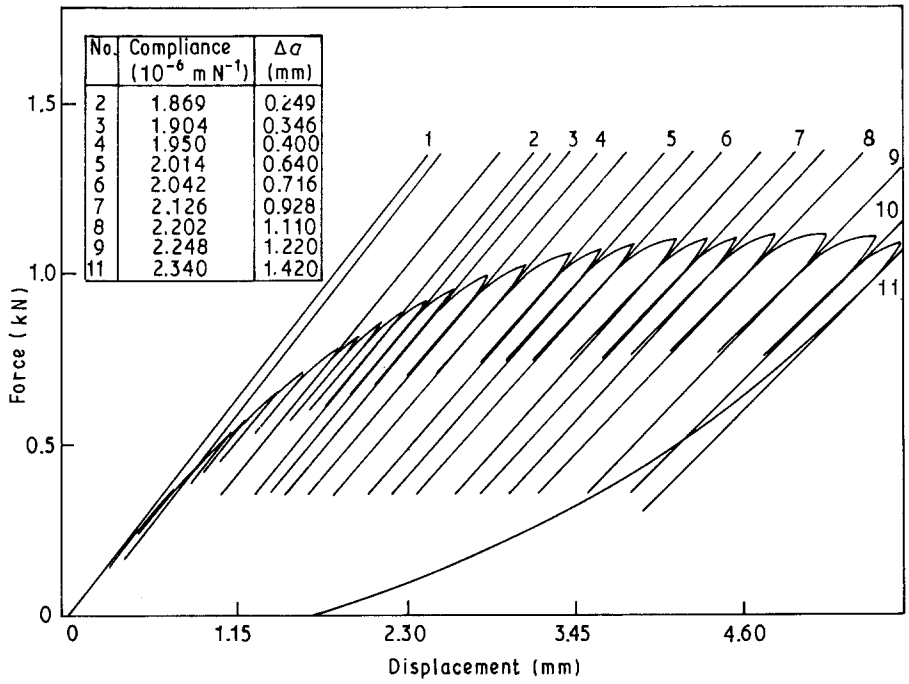

Figure 10 Unload and reload curves for Zytel ST801.

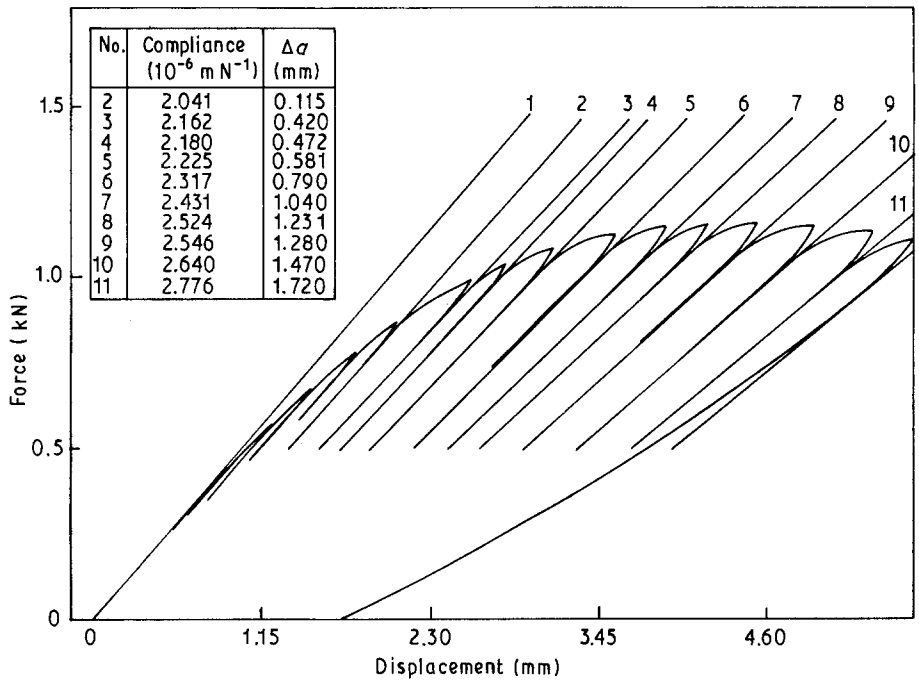

Figure 11 Unload and reload curves for Zytel ST901.

TABLE V Comparison between the measured value of the final crack growth (Δa_m) and the value predicted (Δa_p) from the final unloading compliance curves

Material	Δa_m (mm)	Δa_p (mm)
Zytel ST801	0.43	0.46
Zytel ST801	1.56	1.42
Zytel ST901	2.30	1.84
Zytel ST901	2.45	2.13

first few unloading lines, where $\Delta a = 0$). As may be seen, the lines are drawn to the best linear portion of the unloading curves, ignoring the initial non-linear part which is due to the time-dependent and plasticity effects. Also, there is a slight hysteresis effect which is presumably caused by the viscoelastic nature of the two materials under investigation. As shown in Table V, the unloading compliance predictions of the final crack growth are in good agreement with the measured values, particularly when crack growth is small. Recall that the crack growth measurements were made at the centre of the fracture surface. For large crack growth values this corresponded to the maximum amount of crack extension in the specimen due to the thumbnail shape of the crack front. It is, therefore, expected to have a closer agreement between the Δa_m (measured value) and Δa_p (estimated value) when crack growth is small and the crack front is less curved. Nevertheless, the agreement between these values is very encouraging.

The J-value at each unloading point was calculated using the following relationship (by substituting

TABLE VI Single specimen test results for Zytel ST901 and Zytel ST801

Material	Standard	Resistance curve	J_{IC} (kJ m^{-2})
Zytel ST901	ASTM E813-87	$J = 37.012\,(\Delta a)^{0.712}$	18.51
Zytel ST801	ASTM E813-87	$J = 49.916\,(\Delta a)^{0.745}$	34.61

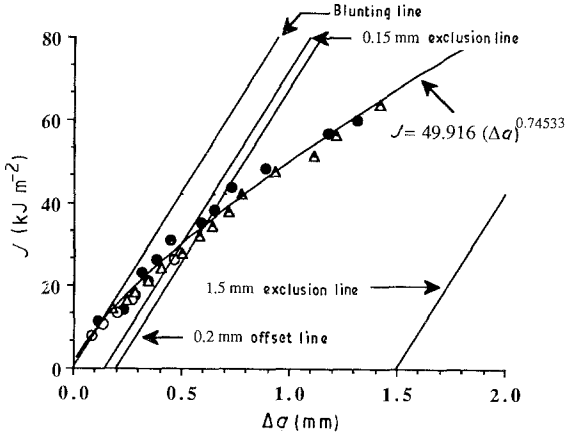

Figure 12 J–Δa curve for Zytel ST801. Data were obtained using the single specimen R-curve method, and analysed according to ASTM E318-87.

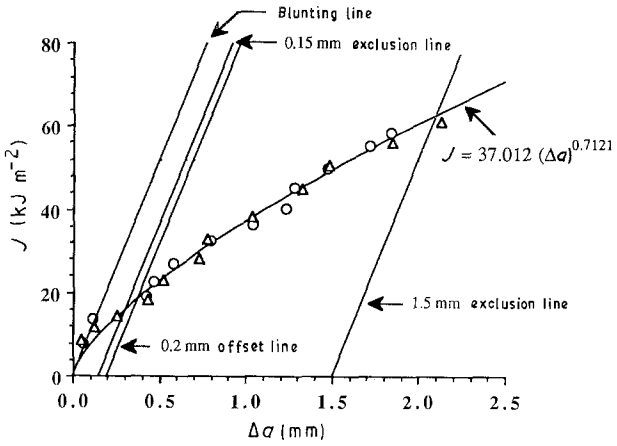

Figure 13 J–Δa curve for Zytel ST901. Data were obtained using the single specimen R-curve method, and analysed according to ASTM E318-87.

$\eta_e = \eta_p = 2$ in Equation 12)

$$J_k = J_{k-1} + \frac{2U_{k,k-1}}{B(W-a)} \tag{23}$$

where $U_{k,k-1} = U_{e(k,k-1)} + U_{p(k,k-1)}$ (the area under the load–loadline displacement record between lines of constant displacement at two consecutive unloading points k and $k-1$). The single specimen J–R curves for the two materials are shown in Figs 12 and 13. The R-curves in these figures were constructed according to the ASTM E813-87 test procedure only. Once again data point spacing is as prescribed by the standard, and J–Δa points show little scatter. A summary of the single specimen test results can be found in Table VI. Essentially, the results of the single specimen test method agree quite well with the results of multi-specimen test method, as shown in Figs 14 and 15.

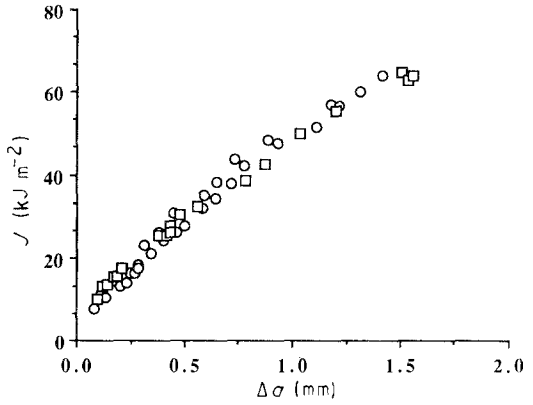

Figure 14 Comparison of the (□) multiple and (○) single specimen R-curves for Zytel ST801.

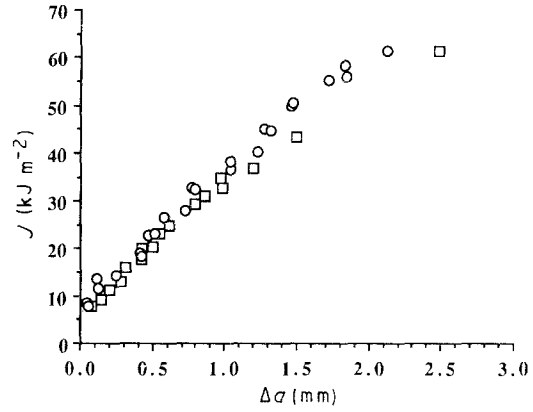

Figure 15 Comparison of the (□) multiple and (○) single specimen R-curves for Zytel ST901.

7. Conclusions

1. The multiple specimen unloading method and the single specimen partial unloading compliance method can be used to generate crack growth resistance J–R curves of toughened nylons. Comparable results are obtained from these two test methods.

2. The value of J_{IC} for the crystalline rubber-toughened nylon (Zytel ST801) was approximately twice the value obtained for the amorphous rubber-toughened nylon. The former material also exhibited a greater resistance to ductile crack growth.

3. J–R curves defined by ASTM E813-87 test procedure gave J_{IC} values which were approximately twice the J_{IC} values obtained by the ASTM E813-81 test procedure.

Acknowledgements

The authors thank DuPont de Nemours and Company, Inc., for their financial support for the work, Drs

D. D. Huang and B. A. Crouch for helpful comments, and Mr W. N. Chung for valuable discussions.

References

1. S. HASHEMI and J. G. WILLIAMS, *J. Mater. Sci.* **19** (1984) 3746.
2. *Idem, ibid.* **20** (1985) 922.
3. ASTM E399-78a, "Standard Test Method for Plane Strain Fracture Toughness of Metallic Materials", 1979 Annual Book of ASTM standards, Part 10 (American Society for Testing and Materials, Philadelphia, Pennsylvania, 1979) p. 540.
4. ASTM E813-81, "Standard Test Method for, J_{IC}, A Measure of Fracture Toughness", 1981 Annual Book of ASTM standards, Part 10 (American Society for Testing and Materials, Philadelphia, Pennsylvania, 1981) p. 810.
5. ASTM E813-87, "Standard Test Method for, J_{IC}, A Measure of Fracture Toughness", 1987 Annual Book of ASTM standards, Part 10 (American Society for Testing and Materials, Philadelphia, Pennsylvania, 1987) p. 968.
6. S. HASHEMI and J. G. WILLIAMS, *Polymer* **27** (1986) 384.
7. *Idem, Polym. Engng Sci.* **26** (1986) 760.
8. *Idem, Plastics Rubber Proc. Appl.* **6** (1986) 363.
9. D. D. HUANG and J. G. WILLIAMS, *J. Mater. Sci.* **22** (1987) 2503.
10. J. G. WILLIAMS and D. D. HUANG, *Polym. Preprints* **26** (1985) 153.
11. M. K. V. CHAN and J. G. WILLIAMS, *Int. J. Fracture* **19** (1983) 145.
12. G. A. CLARK, W. K. ANDREWS and D. W. SCHMIDT, ASTM STP 590 (American Society for Testing and Materials, Philadelphia, Pennsylvania, 1976) p. 27.
13. J. A. JOYCE and J. P. GUDAS, ASTM STP 668 (American Society for Testing and Materials, Philadelphia, Pennsylvania, 1979) p. 451.
14. G. A. CLARK, ASTM STP 743 (American Society for Testing and Materials, Philadelphia, Pennsylvania, 1981) p. 553.
15. J. R. RICE, *J. Appl. Mech. ASME* **35** (1968) 379.
16. J. D. SUMPTER and C. E. TURNER, *Int. J. Fract.* **9** (1973) 320.
17. J. D. LANDES and J. A. BEGLEY, ASTM STP 560 (American Society for Testing and Materials, Philadelphia, Pennsylvania, 1974) p. 170.
18. J. A. KAPP, G. S. LEGER and B. GROSS, ASTM STP 868 (American Society for Testing and Materials, Philadelphia, Pennsylvania, 1985) p. 27.
19. A. BAKKER, *Int. J. Fatigue Fract. Engng Mater. Struct.* **13** (1990) 145.
20. P. C. PARIS, H. TADA, A. ZAHOOR and H. ERNST, ASTM STP 688 (American Society for Testing and Materials, Philadelphia, Pennsylvania, 1979) p.5.

Received 4 December 1989
and accepted 28 March 1990